DOI: 10.1002/adma.200700083

Amphoteric Phosphorus Doping for Stable p-Type ZnO**

By *Arnold Allenic*, *Wei Guo*, *Yanbin Chen*, *Michael Brandon Katz*, *Guangyuan Zhao*, *Yong Che*, *Zhendong Hu*, *Bing Liu*, *Sheng Bai Zhang*, and *Xiaoqing Pan**

Zinc oxide is a wide bandgap semiconductor with potential applications in optoelectronic devices. The greatest challenge for these applications, however, remains the fabrication of reliable and stable p-type ZnO thin films. Here we report stable phosphorus-doped p-type ZnO thin films grown on (0001) sapphire substrates by pulsed laser ablation. While as-deposited films all show n-type conductivity, films grown at 600 °C become p-type after annealing in oxygen atmosphere with a resistivity of 4.9×10^1 Ω cm, a Hall mobility of 1 $cm^2 V^{-1} s^{-1}$, and a hole concentration of 1.3×10^{17} cm^{-3}. Such p-type films have been stable under ambient conditions for 16 months so far without apparent degradation. Transmission electron microscopy reveals that the p-type films consist of a high density of dislocations, which enhance both the solubility of phosphorus and the formation of Zn vacancies to facilitate the n-to-p conversion of electrical conductivity. These studies provide microscopic evidence of the amphoteric nature of the phosphorus dopant in ZnO.

There has recently been an increasing interest in ZnO for applications in optoelectronics such as light emitting diodes, ultraviolet (UV) lasers, and UV light detectors because of its wide bandgap (3.37 eV). In comparison with GaN, ZnO has some obvious advantages for optoelectronic applications due to the availability of single crystal substrates, relatively low growth temperatures (T_G), and a large exciton binding energy (~60 meV).[1] Optically pumped excitonic lasing of ZnO thin films at room temperature (RT) has been reported.[2,3] Lasing effects in ZnO nanowire arrays have been demonstrated,[4] and electroluminescence (EL) has been observed at room temperature in thin-film ZnO homojunctions.[5–7] Although p-type ZnO thin films were reported by several groups, they showed high resistivity and/or poor stability and reproducibility. Thus, the greatest remaining challenge for ZnO optoelectronics is the reproducible fabrication of stable p-type ZnO thin films. Like many other II-VI semiconductors, ZnO has asymmetric doping limits:[8] it can be easily doped n-type,[9] but remains strongly resistant to p-type doping.[10] Though nitrogen is theoretically the most promising acceptor for ZnO, its low solubility and compensation by donors such as hydrogen[11] and Zn interstitials[12] are major obstacles.

As alternatives to N, larger-size group V elements such as P, As, Sb and Bi have been widely studied. Puzzling observations of p-type conductivity in such materials have stimulated theoretical investigations into the electronic structure of the defects induced by P, As or Sb in ZnO. Limpijumnong et al.[13] predicted that under oxygen-rich growth conditions, a complex involving a group V antisite and two zinc vacancies (V_{Zn}) would have a low formation energy, and behave as a shallow acceptor with an ionization energy of 150–160 meV. Lee et al. used the same concept to study phosphorus complexes in ZnO.[14] One of the most important conclusions from these studies is that such group V dopants are amphoteric—acting as a donor as an isolated antisite impurity, but as an acceptor when forming a complex with two V_{Zn}. Although p-type conductivity has been reported,[15–17] little microscopic information on phosphorus and its related defect complex responsible for the p-type conductivity, has emerged.

In this work, we report the fabrication and characterization of stable p-type ZnO films by pulsed laser deposition. We studied microscopic defects induced by phosphorus doping of ZnO and determined the growth and annealing temperatures at which p-type ZnO films can be reproducibly fabricated. The best experimental condition for p-type ZnO is determined to be $T_G = 600$ °C, followed by annealing at $T_A = 600$ °C in O_2 gas. The onset of good p-type conductivity is always accompanied by a considerable increase in the density of dislocations, as revealed by transmission electron microscopy (TEM) studies. Meanwhile, secondary ion mass spectroscopy (SIMS) reveals a significant increase in the solubility of phosphorus. These results suggest that T_G and T_A control the density of dislocations, which in turn controls the solubility of phosphorus. Furthermore, as gettering centers for zinc interstitials, the dislocations also facilitate the formation of zinc vacancies for P_{Zn}–$2V_{Zn}$ acceptors. Our physical insights further allow for the fabrication of P-doped ZnO homojunctions with impressive rectifying characteristics by adjusting only T_G and T_A during processing.

The room temperature electrical properties of different ZnO films are summarized in Table 1. As-deposited P-doped ZnO (PZO) films show n-type conductivity and are more con-

[*] Prof. X. Q. Pan, A. Allenic, W. Guo, Y. B. Chen, M. B. Katz, Dr. G. Y. Zhao
Department of Materials Science and Engineering
The University of Michigan
2300 Hayward Street, Ann Arbor, Michigan 48109 (USA)
E-mail: panx@umich.edu
Dr. Y. Che, Dr. Z. D. Hu, Dr. B. Liu
IMRA America Inc.
1044 Woodridge Avenue, Ann Arbor, Michigan 48105 (USA)
Dr. S. B. Zhang
National Renewable Energy Laboratory
1617 Cole Boulevard, Golden, Colorado 80401 (USA)

[**] This work was supported by NSF/DMR 0308012, IMRA America Inc., and DOE/BES DE-AC36-99GO10337.

 © 2007 WILEY-VCH Verlag GmbH & Co. KGaA, Weinheim WILEY InterScience DISCOVER SOMETHING GREAT

Table 1. RT electrical properties of undoped ZnO and PZO films before and after annealing at 600°C.

Sample	T_G [°C]	Carrier type	Carrier density [cm^{-3}]	Resistivity [Ω·cm]	Mobility [cm^2/V·s]
ZnO as-grown	600	n	7.9×10^{16}	1.7	47
ZnO annealed	600	n	2.4×10^{15}	1.8×10^{2}	14.5
ZnO as-grown	800	n	8.2×10^{16}	6.6×10^{-1}	117
ZnO annealed	800	n	7.3×10^{16}	7.1×10^{-1}	121
PZO as-grown	600	n	3.8×10^{18}	1.5×10^{-1}	11.1
PZO annealed	600	p	1.3×10^{17}	4.9×10^{1}	1
PZO as-grown	800	n	3.4×10^{18}	3.6×10^{-2}	51
PZO annealed	800	n	2.6×10^{18}	5.1×10^{-2}	47

ductive than the corresponding undoped films. PZO films deposited at 800 °C have excellent n-type properties with a resistivity of 3.6×10^{-2} Ω cm, a Hall mobility of 52 $cm^2 V^{-1} s^{-1}$, and electron concentration of 3.4×10^{18} cm^{-3}. Their electrical properties change only slightly after annealing in O_2 at 600 °C. Although the PZO films as grown at 600 °C are n-type, they become p-type after thermal annealing in O_2 at 600 °C. Field-dependent Hall-effect measurements confirm the positive slope of the Hall coefficient. The resulting p-type samples show a resistivity of 4.9×10^{1} Ω cm, a Hall mobility of 1 $cm^2 V^{-1} s^{-1}$, and a hole concentration of 1.3×10^{17} cm^{-3}. Table 2 shows the comparison of the Hall-effect data measured from a p-type film showing the stability of the electrical

Table 2. Comparison of the Hall-effect data measured from a p-type film showing the stability of the electrical properties.

Measurement Date	Hole concentration [cm^{-3}]	Resistivity [Ω·cm]	Mobility [cm^2/V·s]
Aug.–Sept. 2005	5.8×10^{16}–4×10^{17}	41–43	0.3–2.6
Feb. 2007	8.7×10^{16}	36.6	0.49

properties. The first row shows the distribution of Hall measurements averaged over a period of one month. The second row shows the electrical properties of the same sample measured a year and a half later. It is worth mentioning that the latter results fall within the distribution of the initial results.

The phosphorus concentration profiles in PZO deposited at 600 and 800 °C were determined by SIMS measurements. A phosphorus-implanted ZnO sample was used as reference. It was found that P distributes uniformly (3.5×10^{20} cm^{-3}) in p-type films grown at 600 °C. Compared with the nominal doping of the target, this concentration corresponds to a transfer of only 17 % of the phosphorus from the target to the film. The hole/dopant concentration ratio of 3.7×10^{-4} is consistent, to within one order of magnitude, with the measured acceptor activation energy of 150 meV (see below), which yields a ratio of 2.5×10^{-3} at RT. On the other hand, the P concentration in ZnO decreases rapidly when T_G increases. In particular, at $T_G = 800$ °C, there is a significant segregation of P to the film surface, where the dopant concentration is as high as 2×10^{21} cm^{-3}, and to the interface with sapphire substrate, where the phosphorus concentration is 2×10^{20} cm^{-3}. The concentration in the interior of the film is about 6×10^{19} cm^{-3}, so that the electron/dopant concentration ratio is about 5×10^{-2}.

The microstructures of the PZO films were characterized by x-ray diffraction (XRD) and TEM. No impurity phases were found in any of the films. The tilt angles were determined by a Hall-Williamson analysis[18] and the twist angles were determined by ω-scans of off-axis planes in the skew symmetric diffraction geometry. Table 3 summarizes the average mosaic angles and threading dislocation densities. The tilt

Table 3. Tilt angle, twist angle, and densities of threading dislocations for undoped ZnO, n-type PZO, and p-type PZO.

Sample	T_G [°C]	Tilt [arcmin]	Twist [arcmin]	Ns [cm^{-2}]	Ne [cm^{-2}]
n-type PZO	800	10.4	16.2	7.2×10^{8}	4.2×10^{9}
undoped ZnO	800	4.2	5.4	1.2×10^{8}	4.7×10^{8}
p-type PZO	600	39.6	84	1.0×10^{10}	1.1×10^{11}
undoped ZnO	600	13.2	14.1	1.2×10^{9}	3.2×10^{9}

angle corresponds to the out-of-plane lattice bending caused by screw-type dislocations or partial dislocations (with a density of *Ns*) associated with stacking faults with a displacement vector along the *c*-axis, while the twist angle corresponds to the in-plane angular rotation, which is mainly caused by threading dislocations (with a density of *Ne*), according to our cross-sectional TEM studies. The significant increase of both tilt and twist angles with P doping indicates the degradation of the film crystallinity, which agrees with previous studies of PZO.[19]

Both the ϕ-scans and pole figures were taken for all the phosphorus-doped ZnO films. All films studied in this work were grown epitaxially on the substrate without rotational domains. The in-plane orientation of the ZnO film with respect to the sapphire substrate is ZnO-[100] ‖ Al_2O_3-[210]. The vertical line defects in Figure 1a and b are dislocations which originate from the film/substrate interface due to a large lattice mismatch (16.8 %) between ZnO and sapphire and thread to the film surface. It is worth noting that the TEM images of the PZO films at 800 °C (Fig. 1a) and undoped ZnO films at 600 °C show similar densities of dislocations. Figure 1b shows the microstructure of a p-type PZO film at 600 °C. It is evident from Figure 1b that there exists a high density of threading dislocations throughout the film. Besides the lattice mismatch, the low mobility of substitutional phosphorus atoms at the (relatively low) growth temperature of 600 °C could also contribute to the dislocation density, as we have found that the densities of phosphorus dopant and dislocations are directly correlated. The results in Figure 1a and b are in consistence with the results of XRD in Table 3.

Figure 2a is a high-resolution TEM (HRTEM) image showing the atomic structure of the interface between the PZO

 © 2007 WILEY-VCH Verlag GmbH & Co. KGaA, Weinheim

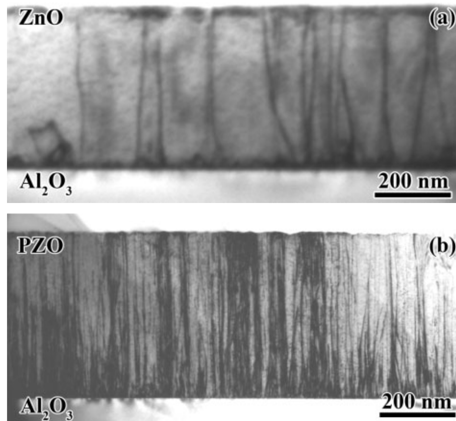

Figure 1. Cross-sectional TEM images of epitaxial PZO films. a) n-type PZO grown at 800 °C; b) p-type PZO deposited at 600 °C. Note that the dislocation density increases with the increase of phosphorus concentration.

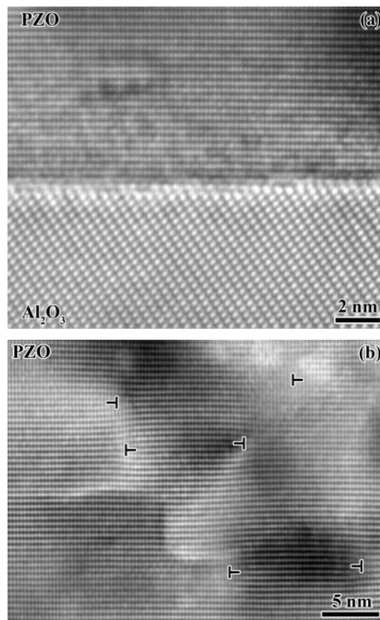

Figure 2. a) Cross-sectional HRTEM image, taken with the electron beam along the [10$\bar{1}$0] direction of ZnO, showing the atomic structure of the interface between the PZO film grown at 600 °C and the sapphire substrate; b) Cross-sectional HRTEM image showing the existence of partial dislocations associated with nanosized stacking faults in the (0001) plane of p-type PZO.

film grown at 600 °C and the sapphire substrate. Although not shown, all the films being studied form atomically sharp interfaces with the substrate, as determined by the HRTEM study. In addition to the threading dislocations in Figure 1b, a high density of partial dislocation loops associated with nano-sized stacking faults also exists in the 600 °C films, as can be seen in the representative HRTEM image in Figure 2b. These defects are expected to form via the condensation of point defects such as zinc interstitials (and oxygen vacancies).[20,21]

Thus, we can attribute the high P solubility in 600 °C films to the existence of a high density of dislocations, which prevent the buildup of strain induced by the P substitution of Zn (the atomic radius of P is 1.06 Å, whereas that of Zn is 1.25 Å). In the theoretical P_{Zn}–$2V_{Zn}$ model for p-type PZO, Zn vacancies play the key role for the conductivity type conversion from n to p. Our observation of dislocation loops with a high concentration here suggests that they facilitate the formation of Zn vacancies by an out-diffusion of Zn interstitials from their cores, as well as the elimination of residual donors such as Zn interstitials and oxygen vacancies by similar out-diffusion processes.

Figure 3a shows the photoluminescence (PL) spectra at 6 K. Undoped ZnO grown at 600 °C [spectrum (i)] has a near band edge (NBE) luminescence dominated by two strong excitonic recombination lines at 368.2 and 368.9 nm due to

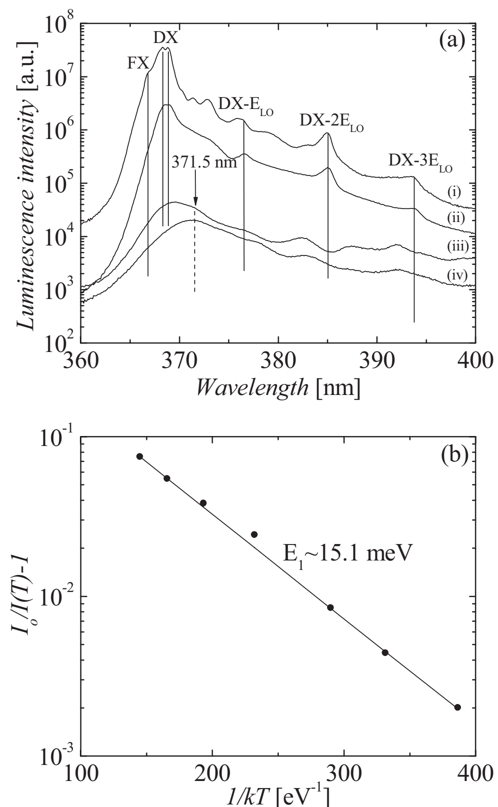

Figure 3. a) PL spectra at 6 K of (i) undoped ZnO grown at 600 °C, (ii) n-type PZO grown at 800 °C, (iii) as-grown PZO at 600 °C, and (iv) p-type PZO grown and annealed at 600 °C. b) Arrhenius plot of the integrated PL intensity of the 371.5 nm line. The circles are the experimental data points and the solid line is the fit.

bound excitons associated with neutral donors (DX). The analysis of the associated two-electron transitions gives two donor activation energies of 30 and 55 meV. There are no obvious differences in the PL spectra of undoped ZnO and n-type PZO grown at 800 °C [spectrum (ii)], consistently with the TEM results, except that only one donor-bound exciton

 © 2007 WILEY-VCH Verlag GmbH & Co. KGaA, Weinheim

could be resolved in n-type PZO. Temperature-dependent studies of the DX line in the n-type PZO film gave a donor activation energy $E_D = 35$ meV. Using this value, we calculated a yield of $\exp(\frac{-E_D}{kT}) = 2.5 \times 10^{-1}$ assuming no compensation. However, from Hall-effect and SIMS measurements, we determined the ionization yield to be $n/[P] = 5 \times 10^{-2}$. This ionization yield is significantly less than 2.5×10^{-1}, suggesting compensation of the free carriers. In contrast, PZO samples grown at 600 °C [spectrum (iii)] show a significantly quenched and broadened NBE luminescence due to the high density of nonradiative defects induced by phosphorous doping. In addition, the luminescence is redshifted from 368.2/368.9 nm to about 369.5 nm, possibly due to the deformation potentials created by phosphorus.

After annealing, the shoulder observed in as-deposited samples near 371.5 nm becomes dominant in p-type PZO [spectrum (iv)]. The temperature dependence of its energy position was found to follow the semi-empirical Varshni equation,[22] $E(T) = E(0) - \alpha\frac{T^2}{T+\beta}$, where $E(0) = 3.346$ eV, $\alpha = 6 \times 10^{-4}$ eV K^{-1}, and $\beta = 300$ K. It should be noted that this temperature dependence does not follow that of the DX, thus excluding the possibility that the 371.5 nm line is a two-electron transition associated with a shallow donor. The temperature dependence of the integrated intensity of the 371.5 nm line (Fig. 3b) was fitted to $\frac{I_0}{I(T)} - 1 = C_1\exp\left(\frac{-E_1}{kT}\right)$. The localization energy E_1 corresponds to the activation energy driving the quenching of the transition at low temperature. From the fitting of the data measured between 20 and 80 K, $E_1 = (15.0 \pm 2.3)$ meV was obtained. The existence of acceptor-bound excitons in ZnO is still under debate and their identification requires further studies. A localization energy of 15 meV is close to that of the I_6 transition that has been assigned to Al. Though heavy doping results in p-type conductivity, the sample is heavily compensated, making it difficult to determine the nature of the 371.5 nm transition unambiguously. Assuming a proportionality constant of 0.1 between the exciton binding energy and the acceptor activation energy E_A,[23] we obtain $E_A = (150 \pm 20)$ meV. This result is in good agreement with density functional theory predictions.[13]

By employing an n-type layer grown at 800 °C and a subsequent p-type layer grown at 600 °C followed by thermal annealing in oxygen, a p-n homojunction was fabricated on both sapphire and resistive single crystal ZnO substrates. Figure 4 shows the *I–V* characteristics of the n-type layer (curve a), p-type layer (curve b) and p-n junction (curve c), exhibiting the clearly defined rectifying behavior of the p-n junction. By fitting the linear segment of the curve under positive bias, we obtain a turn-on voltage of ~5.5 V and an ideality factor of 1.7 ± 0.2. The junction has a breakdown voltage of 13 V with a leakage current that increases slightly under increasing reverse bias. In order to study the stability of the junction, the *I–V* curves across the homojunctions were measured after four and eight months (curves d and e). The measurements

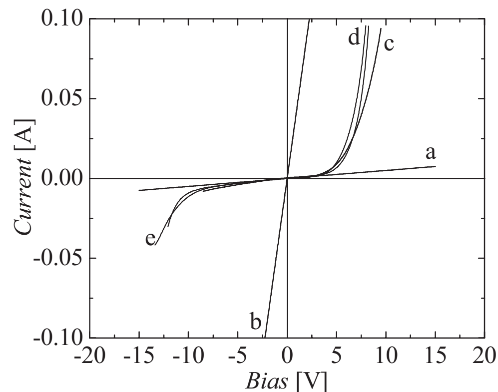

Figure 4. *I–V* characteristics of a) In contacts of the bottom n-type PZO layer, b) Ni/Au contacts of the top p-type PZO layer, respectively. c), d), and e) the rectifying *I–V* characteristics of the corresponding p-n homojunction measured over a period of eight months.

show that the p-n junction behavior has not changed in the eight-month period. Despite the excellent *I–V* characteristic and stability of the junctions, no EL could be observed at room temperature. There are several issues that may prevent the p-n junction from emitting photons. First, there is a trade-off between hole depletion in the p-type PZO film, when its thickness is less than the Debye length, and EL quenching due to the re-absorption or scattering of photons if the layer is too thick. Second, defects at the p-n junction interface may seriously degrade the active region and act as leakage paths. Finally, the mobility of dislocations upon application of a bias may also degrade the p-n junction, as observed in ZnSe-based devices. Thus, the challenges due to the large density of the dislocations and interfacial defects must be dealt with for any ZnO-based optoelectronic devices.

In conclusion, we have successfully fabricated stable p-type epitaxial ZnO thin films and p-n homojunctions with good rectifying behavior by phosphorus doping. This work provides an experimental proof to the amphoteric doping nature of phosphorus in ZnO. The conductivity of our P-doped films can be tuned to either n- or p-type via control of the growth and annealing temperatures, as the growth and annealing conditions control the microscopic quality of the films. Good p-type conductivity is always associated with a considerable increase in the density of dislocations and a significant increase in the solubility (and uniformity in the distribution) of the phosphorus dopant. While the formation of threading dislocations helps the solubility of phosphorus, the formation of dislocation loops during film growth provides a mechanism for zinc vacancy injection and sinks to quench the residual donors in ZnO such as oxygen vacancies and zinc interstitials.

Experimental

Phosphorus-doped ZnO films were fabricated on (0001) sapphire substrates using pulsed laser deposition. Results presented here are solely for films with a thickness of ~0.5 µm. The nominal fraction of

© 2007 WILEY-VCH Verlag GmbH & Co. KGaA, Weinheim

P_2O_5 in the target was 1.0 wt %, the substrate temperatures were 600 and 800 °C, and the O_2 backfill pressure was fixed to 2.7×10^{-2} mbar. Post-growth thermal treatments were carried out under 1 atm O_2 at 600 °C. Indium was used as the ohmic contact to n-type samples, and a Ni/Au bilayer as that to p-type samples. Low-temperature photoluminescence spectra were measured using a 100 mW He-Cd laser ($\lambda = 325$ nm) as the excitation source and a HORIBA Jobin-Yvon 1 m monochromator.

Received: January 10, 2007
Revised: May 15, 2007
Published online: September 21, 2007

[1] Y. Chen, D. Bagnall, T. Yao, *Mater. Sci. Eng. B* **2000**, *75*, 190.
[2] D. M. Bagnall, Y. F. Chen, Z. Zhu, T. Yao, S. Koyama, M. Y. Shen, T. Goto, *Appl. Phys. Lett.* **1997**, *70*, 2230.
[3] M. Kawasaki, A. Ohtomo, I. Ohkubo, H. Koinuma, Z. K. Tang, P. Yu, G. K. L. Wong, B. P. Zhang, Y. Segawa, *Mater. Sci. Eng. B* **1998**, *56*, 239.
[4] M. H. Huang, S. Mao, H. Feick, H. Yan, Y. Wu, H. Kind, E. Weber, R. Russo, P. Yang, *Science* **2001**, *292*, 1897.
[5] A. Tsukazaki, A. Ohtomo, T. Onuma, M. Ohtani, T. Makino, M. Sumiya, K. Ohtani, S. F. Chichibu, S. Fuke, Y. Segawa, H. Ohno, H. Koinuma, M. Kawasaki, *Nat. Mater.* **2005**, *4*, 42.
[6] J. H. Lim, C. K. Kang, K. K. Kim, I. K. Park, D. K. Hwang, S. J. Park, *Adv. Mater.* **2006**, *18*, 2720.
[7] Y. R. Ryu, J. A. Lubguban, T. S. Lee, H. W. White, T. S. Jeong, C. J. Youn, B. J. Kim, *Appl. Phys. Lett.* **2007**, *90*, 131 115.
[8] S. B. Zhang, S. H. Wei, A. Zunger, *J. Appl. Phys.* **1998**, *83*, 3192.
[9] T. Minami, H. Nanto, S. Takata, *Jpn. J. Appl. Phys., Part 2* **1984**, *23*, L280.
[10] C. H. Park, S. B. Zhang, S. H. Wei, *Phys. Rev. B* **2002**, *66*, 073 202.
[11] C. G. Van de Walle, *Phys. Rev. Lett.* **2000**, *85*, 1012.
[12] D. C. Look, G. C. Farlow, P. Reunchan, S. Limpijumnong, S. B. Zhang, K. Nordlund, *Phys. Rev. Lett.* **2005**, *95*, 225 502.
[13] S. Limpijumnong, S. B. Zhang, S. H. Wei, C. H. Park, *Phys. Rev. Lett.* **2004**, *92*, 155 504.
[14] W. J. Lee, J. Kang, K. J. Chang, *Phys. Rev. B* **2006**, *73*, 024 117.
[15] K. K. Kim, H. S. Kim, D. K. Hwang, J. H. Lim, S. J. Park, *Appl. Phys. Lett.* **2003**, *83*, 63.
[16] S. Jang, J. J. Chen, B. S. Kang, F. Ren, D. P. Norton, S. J. Pearton, J. Lopata, W. S. Hobson, *Appl. Phys. Lett.* **2005**, *87*, 222 113.
[17] F. X. Xiu, Z. Yang, L. J. Mandalapu, J. L. Liu, W. P. Beyermann, *Appl. Phys. Lett.* **2006**, *88*, 052 106.
[18] G. K. Williamson, W. H. Hall, *Acta Metall.* **1953**, *1*, 22.
[19] Y. W. Heo, S. J. Park, K. Ip, S. J. Pearton, D. P. Norton, *Appl. Phys. Lett.* **2003**, *83*, 1128.
[20] D. Gerthsen, D. Livitnov, T. Gruber, C. Kirchner, A. Waag, *Appl. Phys. Lett.* **2002**, *81*, 3972.
[21] H. P. Sun, X. Q. Pan, X. L. Du, Z. X. Mei, Z. Q. Feng, Q. X. Xue, *Appl. Phys. Lett.* **2004**, *85*, 4385.
[22] Y. P. Varshni, *Physica* **1967**, *34*, 149.
[23] J. R. Haynes, *Phys. Rev. Lett.* **1960**, *4*, 361.

 © 2007 WILEY-VCH Verlag GmbH & Co. KGaA, Weinheim